Article

Journal of
Nanoscience and Nanotechnology
Vol. 15, 2067–2078, 2015
www.aspbs.com/jnn

Three Arginine-Rich Cell-Penetrating Peptides Facilitate Cellular Internalization of Red-Emitting Quantum Dots

Betty R. Liu[1], Hwei-Hsien Chen[2,*], Ming-Huan Chan[3], Yue-Wern Huang[4], Robert S. Aronstam[4], and Han-Jung Lee[1,*]

[1] *Department of Natural Resources and Environmental Studies, National Dong Hwa University, Hualien 97401, Taiwan*
[2] *Center for Neuropsychiatric Research, National Health Research Institutes, Miaoli 35053, Taiwan*
[3] *Institute of Neuroscience, National Chengchi University, Taipei 11605, Taiwan*
[4] *Department of Biological Sciences, Missouri University of Science and Technology, Rolla, MO 65409-1120, USA*

Nanoparticles, such as semiconductor quantum dots (QDs), have been found increasing use in biomedical diagnosis and therapeutics because of their unique properties, including quantum confinement, surface plasmon resonance, and superparamagnetism. Cell-penetrating peptides (CPPs) represent an efficient mechanism to overcome plasma membrane barriers and deliver biologically active molecules into cells. In this study, we demonstrate that three arginine-rich CPPs (SR9, HR9, and PR9) can noncovalently complex with red light emitting QDs, dramatically increasing their delivery into living cells. Zeta-potential and size analyses highlight the importance of electrostatic interactions between positive-charged CPP/QD complexes and negative-charged plasma membranes indicating the efficiency of transmembrane complex transport. Subcellular colocalization indicates associations of QD with early endosomes and lysosomes following PR9-mediated delivery. Our study demonstrates that nontoxic CPPs of varied composition provide an effective vehicle for the design of optimized drug delivery systems.

Keywords: Cell-Penetrating Peptides, Nanoparticles, Polyarginine, Protein Transduction, Quantum Dots.

1. INTRODUCTION

Quantum dots (QDs) are colloidal, inorganic semiconductor nanoparticles with unique physicochemical properties.[1] QDs are excellent alternatives to organic dyes and fluorescent proteins for various cellular and biomedical imaging applications due to their high photoluminescent quantum efficiency, narrow emission spectral band, tunability, and photostability.[1–4] QDs also provide high quality deep tissue imaging using two-photon excitation microscopes.[5] However, some drawbacks of QDs restrict their applicability for diagnosis and therapeutics. For instance, QDs dispersed in nonpolar solvents gradually aggregate and lose their fluorescence intensity, even in the dark.[6] QDs enter cells very slowly and tend to become trapped in endosomes or other vesicles following cellular entry.[3,4,7] Therefore, methods to improve QD solubility, cellular uptake, and biodelivery are needed. Microinjection, electroporation, and liposome-based transduction have been used to increase QD transduction efficiency.[6,8] Conjugation with polymer ligands has emerged as an important tool in overcoming transduction limitations.[9]

Cell-penetrating peptides (CPPs), also called protein transduction domains (PTDs), are a group of short, highly basic peptides that are capable of penetrating cell membrane and delivering biologically active molecules into cells.[10–13] CPPs may be cationic, amphipathic, or hydrophobic.[14] Our previous studies demonstrated that CPPs can deliver biomolecules into cells following association in covalent (CPT),[15–19] noncovalent (NPT),[20–31] or mixed covalent and noncovalent protein transductions (CNPT) manners.[32,33] Cargoes that can be carried by CPPs include proteins, DNAs, RNAs, peptide nucleic acids (PNAs), small molecular drugs, inorganic particles, and liposomes.[34–36] CPPs can deliver cargoes to both prokaryocytes and eukaryocytes.[15–33]

Synthetic R9 (SR9) peptides destabilize the plasma membrane creating transient pores for cellular penetration.[37] Histidine-rich R9 (HR9; CH5-R9-H5C)

*Authors to whom correspondence should be addressed.

consists of polyhistidine and nona-arginine (R9) sequences flanked by two cysteine residues.[26–30] Addition of polyhistidine and cysteine residues to CPPs endows the complexes with endosomolytic properties and increases the gene expression of DNAs carried by CPPs.[38] The penetration accelerating sequence (Pas) is a synthetic peptide (FFLIPKG) derived from the cleavable sequence (GKPILFF) of a lysosomal aspartyl protease.[39,40] Pas nona-arginine (PR9; FFLIPKG-R9) is comprised of Pas and the R9 consensus segment.[26–28,30] Addition of Pas to octa-arginine (R8), denoted as PasR8, enhances the efficiency of intracellular delivery of bioactive peptides by promoting endosomal escape.[39] For instance, a retro-inverso peptide containing Pas, a CPP, and the p53 C-terminal 22-amino-acid peptide induces p53-dependent autophagic cell death.[40]

To improve the cellular uptake efficiency of QDs, QDs can be functionalized with CPPs by either covalent conjugation or noncovalent interactions.[41] Covalent coupling methods tend to produce larger nanoparticles (10–50 nm) with greater colloidal stability,[42] increased solubility, and efficiency of transduction delivery.[43] In contrast, noncovalent approaches are simple and produce smaller nanoparticles (< 10 nm) with weaker binding between peptides and QDs, and less colloidal stability.[44] Studies have used QDs whose surfaces have been modified by covalent[42,45,46] or noncovalent[47–55] linkages with CPPs (referred to as CPP-QD or CPP/QD, respectively). Arginine-rich CPPs have recently been demonstrated to deliver green-emitting QDs into cells.[49–55] Red-emitting QDs are of particular interest for *in vivo* biomedical applications due to deep tissue penetration of red light. However, very few investigations have focused on cellular delivery of red-emitting QDs by IR9.[53] In this report, we characterize the physical properties of noncovalent interactions between three arginine-rich CPPs (SR9, HR9, and PR9) and red-emitting QDs. The subcellular localizations and cytotoxicity of CPP/QD complexes were also investigated.

2. EXPERIMENTAL DETAILS

2.1. QDs and Peptides

Carboxyl-functionalized CdSe/ZnS QDs eFluor 625NC (red luminescent QDs; herein denoted as QD) possess a maximal emission peak wavelength of 625 nm (eBioscience, Affymetrix, San Diego, CA, USA). Three arginine-rich CPPs, SR9 (R9), HR9 (CH5-R9-H5C), and PR9 (FFLIPKG-R9) were synthesized by Genomics Co. (Taipei, Taiwan).[26–30]

2.2. Gel Retardation Assay

To determine noncovalent interactions between CPPs and QDs, various amounts of SR9 (from 0 to 960 μM), HR9, and PR9 (from 0 to 480 μM) were mixed with 2 μM of QDs in phosphate buffered saline (PBS) and then incubated for 2 h at 37 °C. CPP/QD complexes

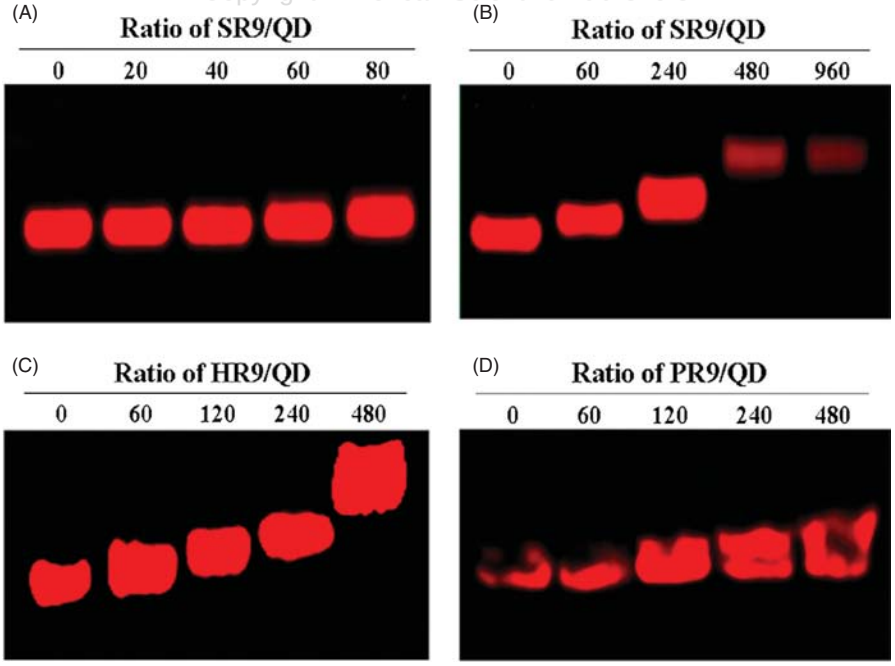

Figure 1. Gel retardation of CPP/QD complexes. (A), (B) Gel retardation assays of SR9/QD complexes prepared at different combination ratios: 0 (QD alone), 20, 40, 60, 80, 240, 480, and 960. (C) Gel retardation of HR9/QD complexes prepared at molecular ratios of 0, 60, 120, 240, and 480. (D) Gel retardation of PR9/QD complexes prepared at molecular ratios of 0, 60, 120, 240, and 480. After incubation at 37 °C for 2 h, the mixtures were analyzed by electrophoresis on a 0.5% agarose gel. Fluorescence of QD was visualized using a Typhoon FLA 9000 biomolecular imager.

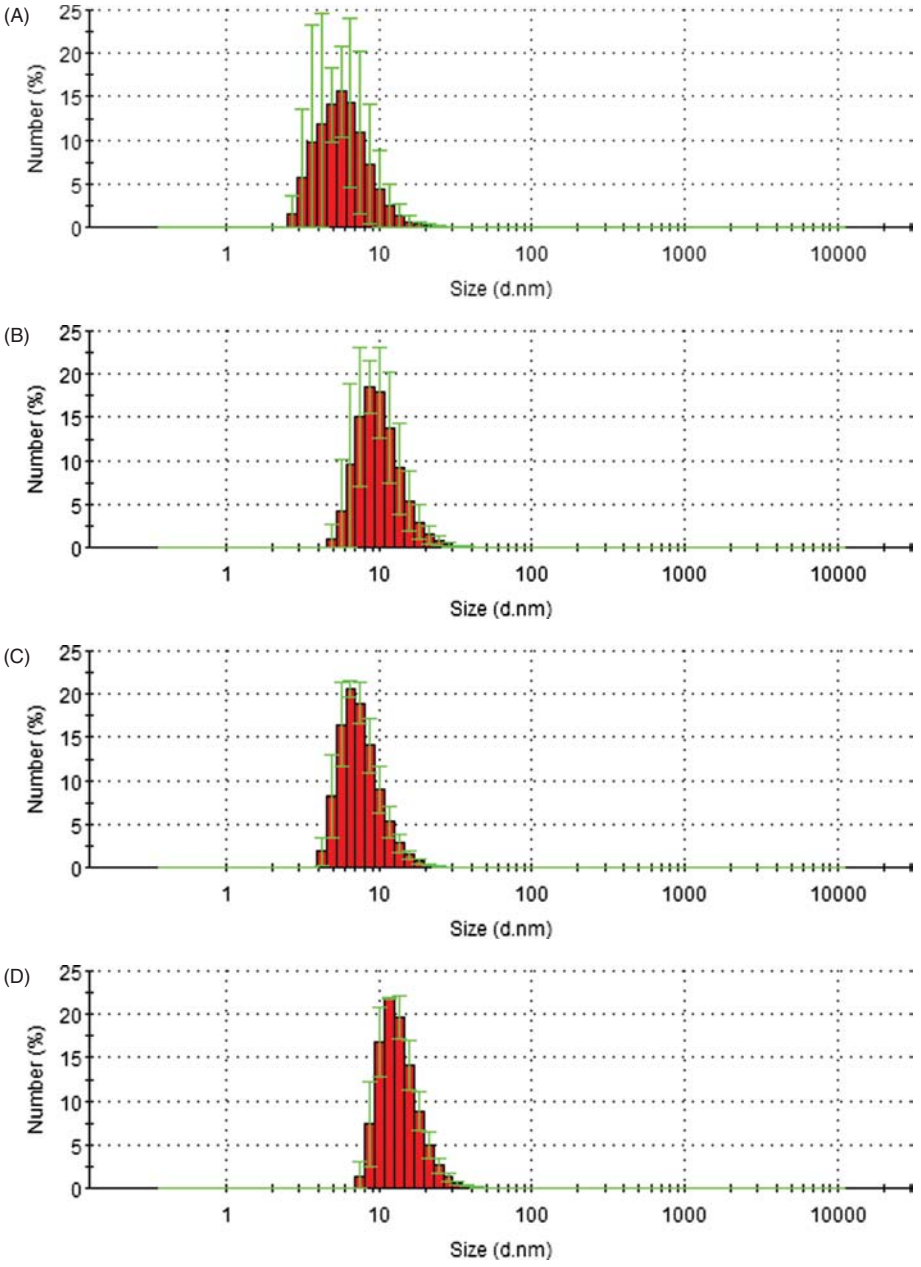

Figure 2. Particle sizes of CPP/QD complexes measured by a Zetasizer. The sizes of QD alone (A), and SR9/QD (B), HR9/QD (C), and PR9/QD (D) complexes prepared at a molecular ratio of 480 are shown.

prepared at molecular ratios from 0 to 960 were analyzed by electrophoresis on a 0.5% agarose gel (Multi ABgarose, Thermo Fisher Scientific, Waltham, MA, USA) in 0.5× TAE buffer (40 mM of Tris-acetate and 1 mM of EDTA, pH 8.0) at 100 V for 40 min.[47] Images were captured using a Typhoon FLA 9000 biomolecular imager (GE Healthcare, Piscataway, NJ, USA) with the excitation wavelength at 605 nm of a LD laser and emission wavelengths above 605 nm using a LPB filter. Data were analyzed using ImageQuant TL 7.0 software (GE Healthcare).

2.3. Particle Size and Zeta-Potential Measurement

CPPs (12.4 μM of SR9, HR9, or PR9) and 100 nM of QDs were separately dissolved in double deionized water. The QDs were then mixed with SR9, HR9, or PR9 at a molecular ratio of 480. Each solution was equilibrated at 25 °C for 120 sec. The sizes and zeta-potentials of QDs or

CPP/QD complexes were analyzed using a Zetasizer Nano ZS (Malvern Instruments Ltd., Malvern, Worcestershire, UK) equipped with Zetasizer software 6.30.[51, 53]

2.4. Cell Culture

Human bronchoalveolar carcinoma A549 cells (American Type Culture Collection, Manassas, VA, USA; CCL-185) were cultured in Roswell Park Memorial Institute (RPMI) 1640 medium (Gibco, Invitrogen, Carlsbad, CA, USA) supplemented with 10% (v/v) bovine serum (Gibco) in a humidified incubator with 5% CO_2 at 37 °C.[20]

2.5. Delivery of CPP/QD Complexes Into Cells

To analyze noncovalent transductions between CPPs and QDs, CPPs (SR9, HR9, or PR9) were mixed with QDs at a molecular ratio of 480 for 2 h. Following complex formation, the mixtures were incubated with A549 cells for 1 and 24 h at 37 °C. An optimal ratio of CPP/QD was chosen for subsequent study of transduction kinetics. Accordingly, kinetic studies used 100 nM of QDs alone or 100 nM of QDs mixed with 48 μM of SR9, HR9, or PR9, followed by incubation with A549 cells for a period of 0–5 h at 37 °C.

2.6. Subcellular Colocalization

To study subcellular colocalizations, Hoechst 33342, LysoSensor Green DND-153 (Invitrogen), and mouse fluorescein isothiocyanate (FITC)-conjugated anti-human early endosome antigen 1 protein (EEA1) antibody (BD Biosciences, Franklin Lakes, NJ, USA) were used to visualize nuclei, lysosomes, and early endosomes, respectively.[47, 49] Cells were treated with CPP/QD complexes for 0.5–5 h at 37 °C, and then fixed with 3.7% formaldehyde followed by organelle-marker staining according to the manufacturers' instructions.

2.7. Fluorescent and Confocal Microscopy

Fluorescent and bright-field images were recorded using an Olympus IX70 inverted fluorescent microscope (Olympus, Center Valley, PA, USA)[46] or a BD Pathway 435 System (BD Biosciences).[50] Excitation wavelengths were 377/50 nm, 482/35 nm, and 543/22 nm for blue, green, and red fluorescence, respectively. Emission filters were at 435LP (long-pass), 536/40 nm and 593/40 nm for blue, green, and red fluorescent channels, respectively. Intensities of fluorescent signals were quantified using UN-SCAN-IT software (Silk Scientific, Orem, UT, USA). Bright-field microscopy was used to assess cell morphology.

2.8. Cytotoxicity Measurement

Cells were treated with 0–100 μM of CPPs for 24 h at 37 °C. At the end of the experiment, cell medium was removed, and cells were then washed several times with PBS. Cell viability was determined using the sulforhodamine B (SRB) assay.[32] Cells treated with PBS and 100% dimethyl sulfoxide (DMSO) served as negative and positive controls, respectively.

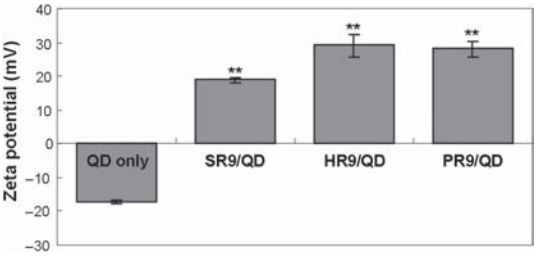

Figure 3. Zeta-potentials of QDs and CPP/QD complexes. CPPs were complexed with QD at a molecular ratio of 480. Significant differences at $P < 0.01$ (**) are indicated. Data in each group are presented as mean ± SD from 3 independent experiments.

2.9. Statistical Analysis

Data are presented as mean ± standard deviation (SD). Mean values and SDs were calculated from at least three independent experiments with triplicate determinations in each treatment group. Statistical comparisons between the control and treated groups were performed by the Student's *t*-test. The level of statistical significance was set at $P < 0.01$ (**).

3. RESULTS

3.1. *In Vitro* Interactions Between CPPs and QDs

Gel retardation analyses were performed to determine whether CPPs form stable complexes with QDs. Three CPPs (SR9, HR9, and PR9) were incubated with QDs at different CPP/QD ratios. SR9, HR9, and PR9 interacted with QDs noncovalently, and the mobility shifts of CPP/QD complexes reflected the amount of CPPs added (Fig. 1). Complexes were completely retarded at CPP/QD ratios of 480 or above. These results indicate that CPPs can interact with QDs to form stable, noncovalent CPP/QD complexes. The optimal combination ratio of CPP versus QD was 480; accordingly, and this ratio was used in subsequent experiments.

3.2. Characteristics of CPP/QD Complexes

To analyze the sizes of complexed particles, QDs and CPP/QD complexes were measured using a Zetasizer. The QD core was approximately 5.6 nm in diameter (Fig. 2(A)). Addition of CPPs to QDs increased the diameters of SR9/QD, HR9/QD, and PR9/QD complexes prepared at a molecular ratio of 480 to about 10.1, 6.5, and 11.7 nm (Figs. 2(B)–(D)), respectively.

The surface charges of QD and CPP/QD complexes prepared at a molecular ratio of 480 were measured using a Zetasizer. QDs exhibited negative charges (−17.3 ± 0.6 mV), while three SR9/QD, HR9/QD, and PR9/QD complexes displayed positive charges (18.9 ± 0.8,

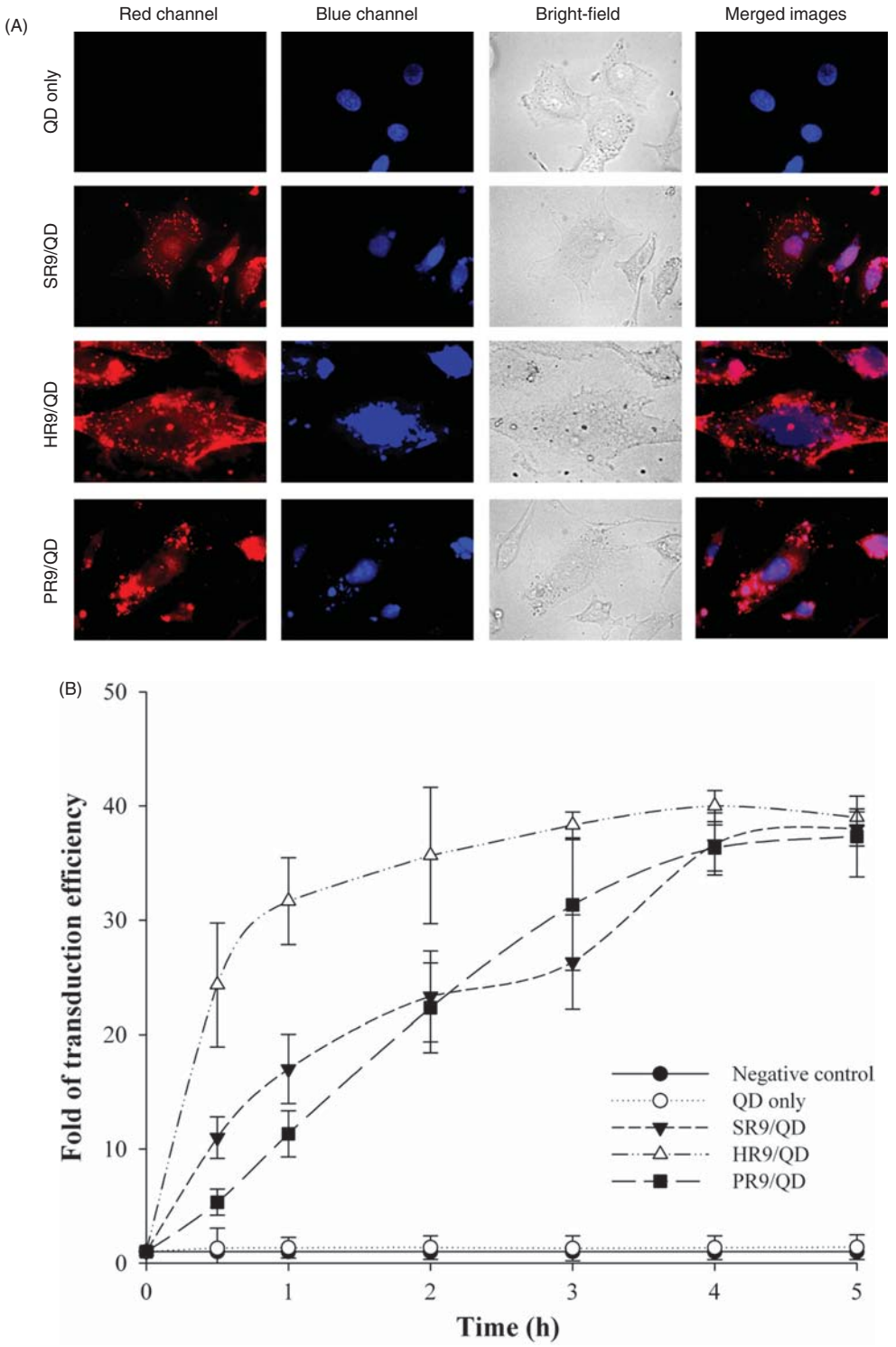

Figure 4. Kinetics of CPP-mediated QDs delivery into A549 cells. (A) CPP-mediated QD delivery into cells. Cells were treated with QD alone, or SR9/QD, HR9/QD, or PR9/QD complexes prepared at a molecular ratio of 480 for 1 h and then stained with Hoechst 33342. (B) Kinetics of the cellular internalization of CPP/QD complexes. Cells were treated with QD alone, or SR9/QD, HR9/QD, or PR9/QD complexes prepared at a molecular ratio of 480 for 0 to 5 h. Fluorescent intensities were quantified from microscopic images using UN-SCAN-IT software. Data are presented as mean ± SD from 7 independent experiments in each treatment group.

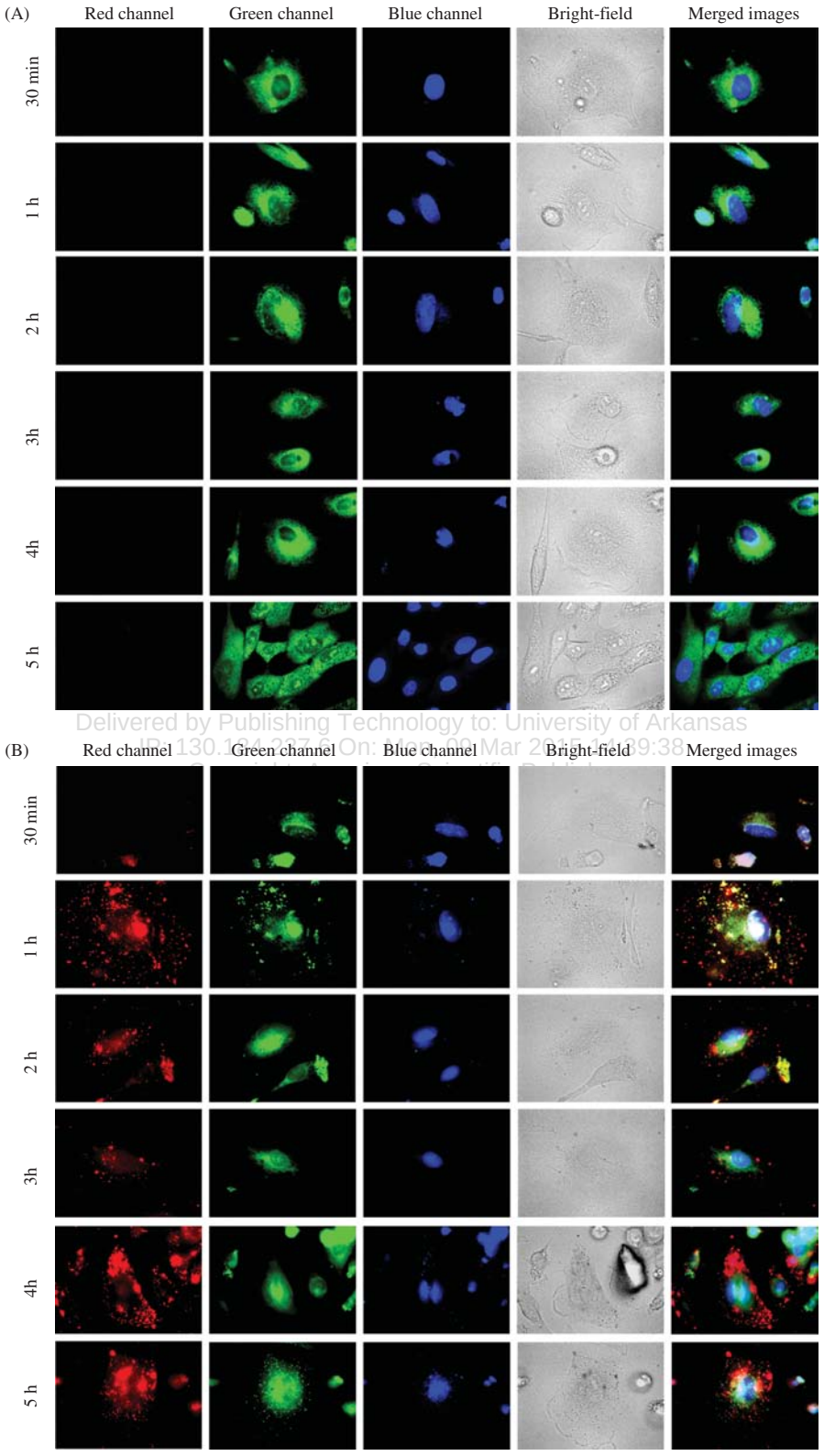

Figure 5. Continued.

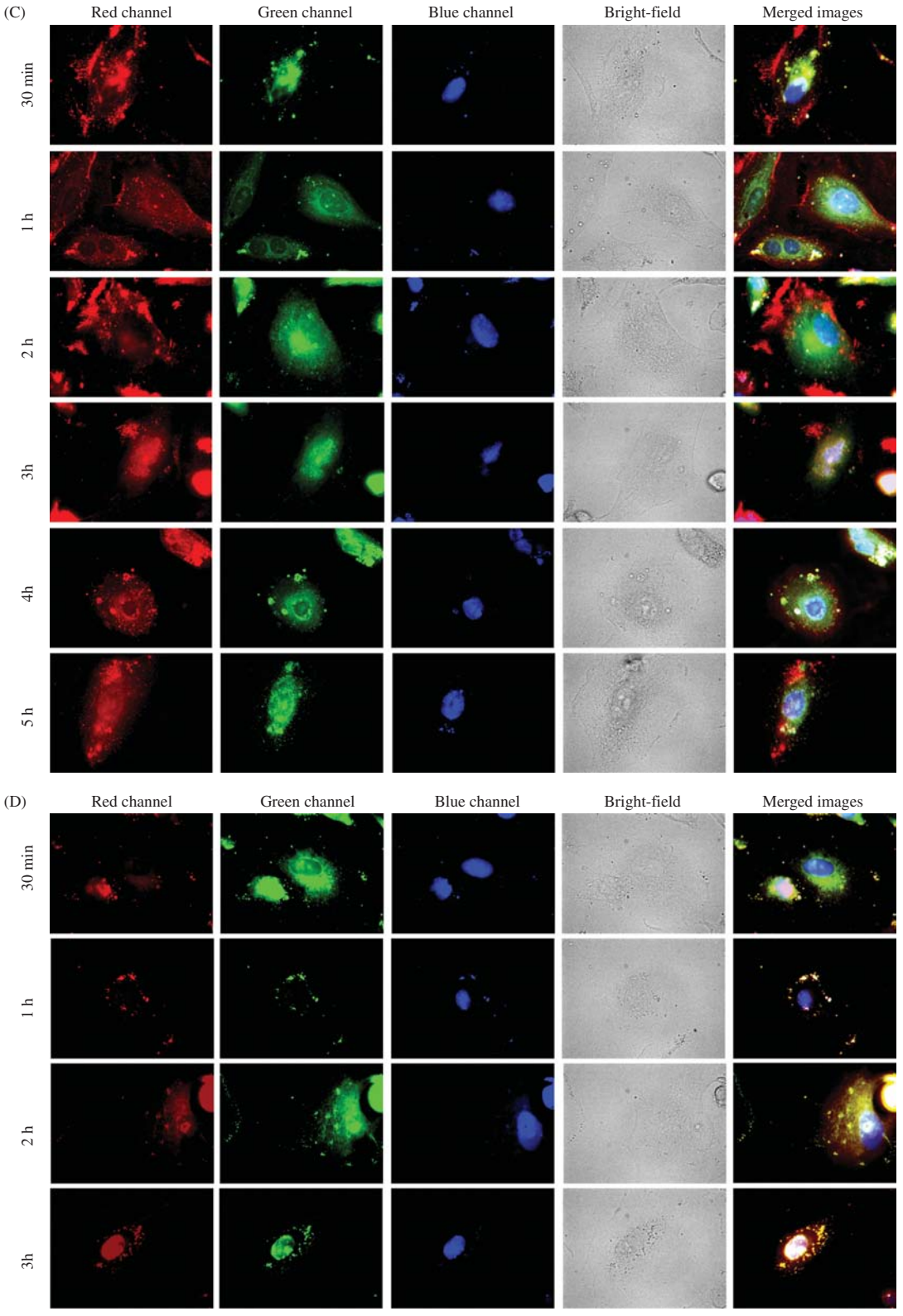

Figure 5. Continued.

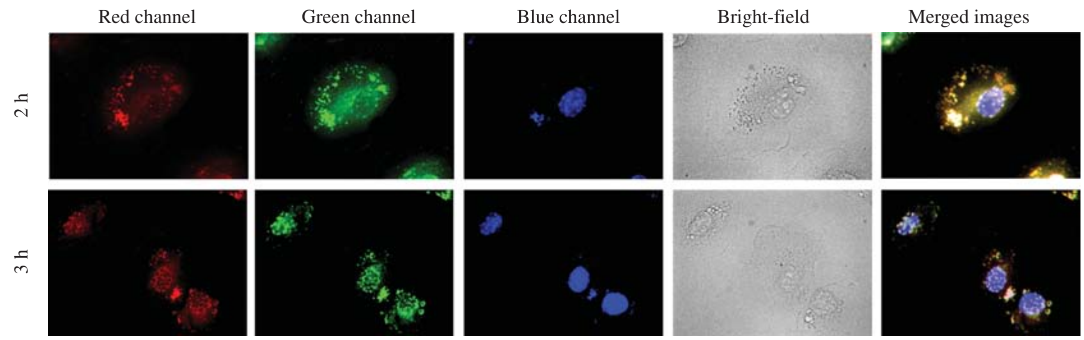

Figure 5. Colocalization of CPP/QD complexes with lysosomes. A549 cells were treated with QD alone (A), or SR9/QD (B), HR9/QD (C), and PR9/QD (D) complexes for various periods of time. The cells were harvested at 30 min and 1–5 h, and stained with LysoSensor and Hoechst. Red, green, and blue fluorescent channels revealed the distributions of QDs, lysosomes, and nuclei, respectively. Overlaps between QDs and organelle trackers exhibit yellow color in merged red and green fluorescent images, while overlaps between QDs and nuclei exhibit violet color in merged red and blue fluorescent images. Cell morphologies were shown in bright-field images. Images were obtained using a BD Pathway 435 System at a magnification of 600×.

29.1 ± 3.4, and 28.1 ± 2.4 mV, respectively) (Fig. 3). This suggests that electropositive charges of CPP/QD complexes are an important factor for transport across the negative-charged cytoplasmic membrane of A549 cells.

3.3. Intracellular Delivery of CPP/QD Complexes

To demonstrate the transduction ability of CPPs, cells were treated with red-emitting QDs or SR9/QD, HR9/QD, or PR9/QD complexes prepared at a molecular ratio of 480 for 1 h, and then stained with Hoechst 33342. Red fluorescence was detected in cells exposed to CPP/QD complexes, but not QDs alone (Fig. 4(A)). To investigate the kinetics of cellular internalization of CPP/QD complexes, cells were treated with QDs or SR9/QD, HR9/QD, or PR9/QD complexes for 0 to 5 h. After 1 h, HR9 complexes demonstrated higher QD transduction than SR9 and PR9 complexes, and HR9-mediated transduction remained higher than transduction mediated by SR9 and PR9 for 4 h (Fig. 4(B)). After 5 h, however, QD transduction efficiencies mediated by SR9, HR9, and PR9 were similar (Fig. 4(B)).

3.4. Subcellular Distributions of CPP/QD Complexes

To determine the subcellular localizations of CPP-delivered QDs, cells were treated with either QDs alone or with CPP/QD complexes, and then stained with the organelle-specific fluorescent markers Hoechst 33342 and LysoSensor Green DND-153 to visualize nuclei and lysosomes, respectively. Cells treated with QDs alone did not accumulate QDs (Fig. 5(A)). Merged images showed that QDs did not associate with nuclei (Figs. 5(B)–(D)) of many cells after transduction delivery. In addition, there was no colocalization of SR9/QD (Fig. 5(B)) or HR9/QD (Fig. 5(C)) complexes with lysosomes. However, some yellow spots were observed in the merged images of PR9/QD groups at 2–5 h treatment (Fig. 5(D)), indicating possible association of QDs with lysosomes after PR9-delivery. These results suggest that internalization of PR9/QD complexes involves endocytosis.

To investigate possible association of CPP/QD complexes with early endosomes, cells were treated with QDs alone or CPP/QD complexes, followed by staining with Hoechst 33342 and FITC-conjugated anti-human EEA1 antibody to visualize nuclei and early endosomes, respectively. Some yellow spots were observed in the merged images of both SR9/QD and PR9/QD groups (Fig. 6(A)) after 1 h transduction delivery. QDs gradually associated with early endosomes (Fig. 6(B)) from 1 to 5 h after PR9-mediated delivery, indicating possible association of PR9/QD with early endosomes.

3.5. Cytotoxicity of CPPs

Exposure to CPPs (0–100 μM) for 24 h at 37 °C at concentrations up to 100 μM did not reduce cell viability (Fig. 7).

4. DISCUSSION

We demonstrated that SR9, HR9, and PR9 interact with QD nanoparticles to form stably noncovalent complexes *in vitro*. Three arginine-rich CPPs facilitated the delivery of noncovalently-associated QDs into human cells. Zeta-potential and size analyses revealed the importance of electrostatic interactions between CPP/QD complexes and plasma membranes. Subcellular colocalizations indicated that PR9/QD complexes stay in early endosomes and lysosomes after transduction delivery. Finally, none of the three arginine-rich CPPs were cytotoxic. These results suggest that these CPPs may be ideal vectors for delivery of diagnostic and pharmaceutical molecules.

The core of a red-emitting QD is approximately 5.6 nm in diameter. Addition of HR9 to QD increased the size of HR9/QD complexes slightly to about 6.5 nm, while addition of SR9 and PR9 doubled the sizes of SR9/QD

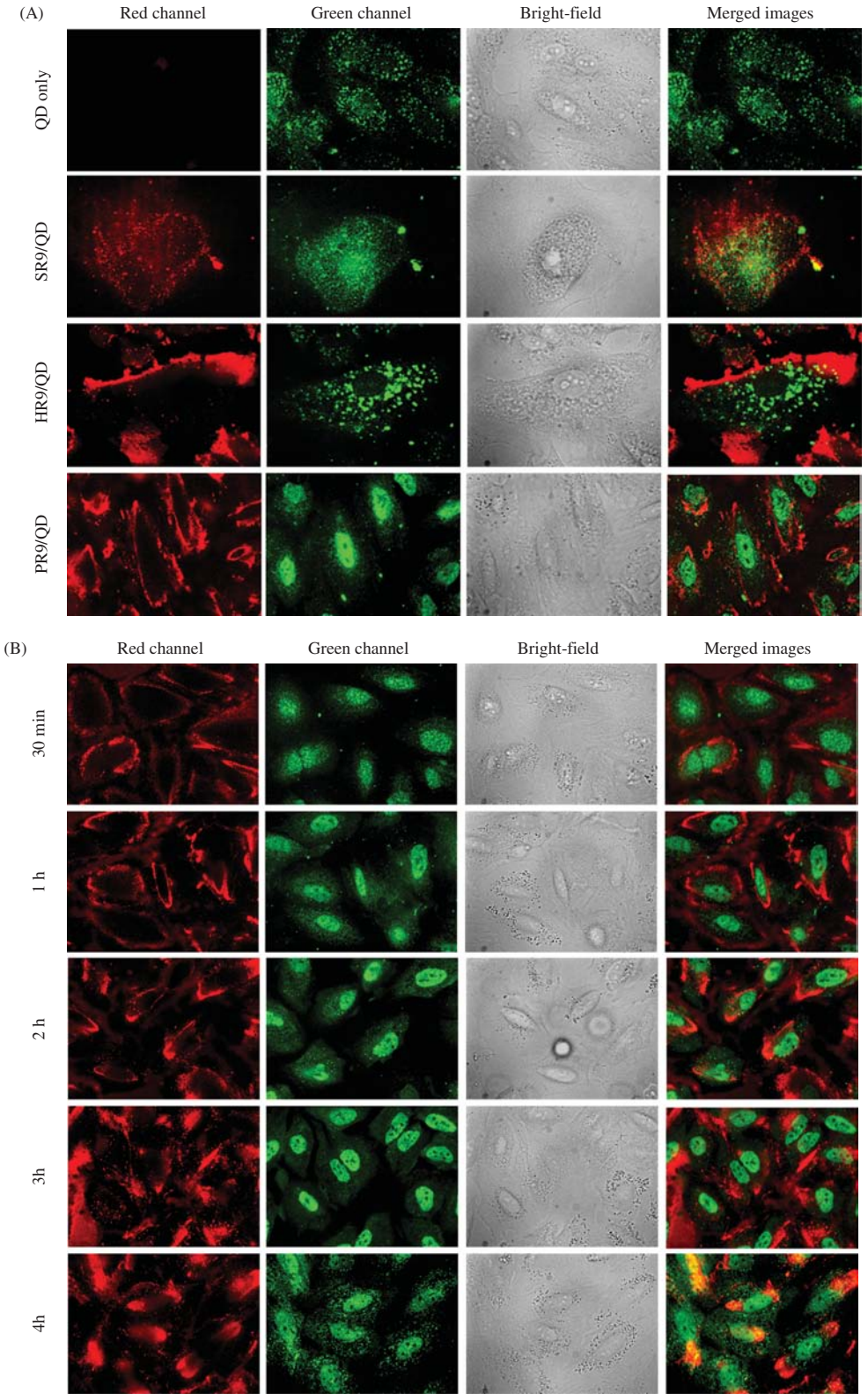

Figure 6. Continued.

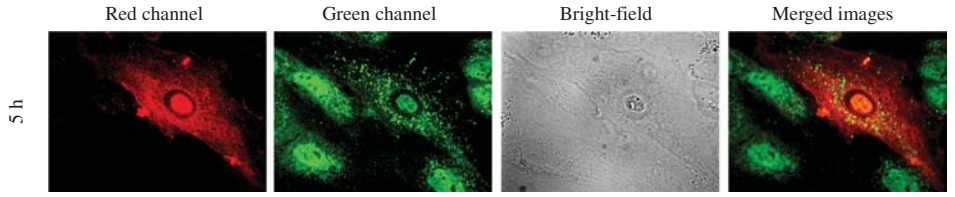

Figure 6. The intracellular trafficking of CPP/QD complexes. (A) Colocalization of CPP/QD complexes with early endosomes. The cells were treated with QD alone, or SR9/QD, HR9/QD, and PR9/QD complexes for 1 h, and then stained with FITC-conjugated anti-human EEA1 antibody. (B) The intracellular trafficking of PR9/QD complexes. The cells were treated with PR9/QD complexes for various periods of time. Cells were harvested at 0.5–5 h, and then stained with FITC-conjugated anti-human EEA1 antibody. Red and green fluorescence revealed the distributions of QDs and early endosomes, respectively. Overlaps between QDs and organelle trackers exhibit yellow color in merged Red and green fluorescent images. Cell morphologies are shown in bright-field images. Images were obtained using a BD Pathway 435 System at a magnification of 600×.

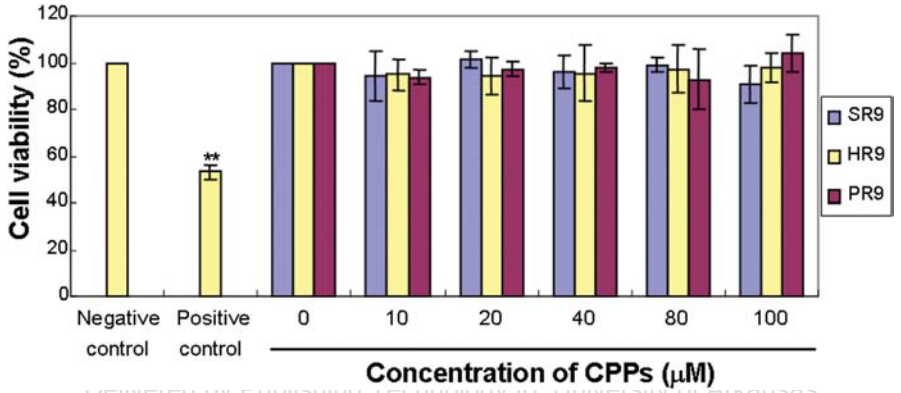

Figure 7. CPP cytotoxicity. Cells were incubated with 0, 10, 20, 40, 80, and 100 μM of SR9, HR9, or PR9 for 24 h, respectively. The SRB assay was used for cytotoxic analysis. Cells treated with PBS and 100% DMSO served as negative and positive controls, respectively. Significant differences at $P < 0.01$ ($**$) are indicated. Data are presented as mean $\pm$ SD from 3 independent experiments.

and PR9/QD complexes. This information indicates that HR9/QD complexes are more compact in structure than SR9/QD and PR9/QD complexes, in agreement with our earlier observation that addition of CPPs (SR9, HR9, and PR9) increases the size of green-emitting QDs (2.0 ± 0.1 nm) to about 15.7 ± 1.1 nm in diameter.[51]

Although CPPs have received a great deal of attention as promoters of cell delivery, the exact cellular uptake pathways of CPPs are still not fully understood. The current understanding is that CPPs utilize multiple pathways for cellular entry.[56,57] Endocytosis and direct membrane translocation appear to be two major routes for CPP transduction. Endocytosis encompasses multiple energy-dependent pathways, including phagocytosis and pinocytosis.[57,58] Pinocytosis can be further divided into nonclassical macropinocytosis, clathrin-dependent, caveolin-dependent, and clathrin/caveolin-independent pathways.[58] Direct membrane translocation involves an energy-independent pathway that includes pore formation, inverted micelle formation, carpet-like perturbation, and membrane thinning model.[29,59] CPPs at high concentrations or with primary amphipathic structures preferably enter cells via this energy-independent pathway.[60] Our previous results indicated that the mechanisms of cellular uptake of SR9/QD,[47,48] HR9/QD,[49] and PR9/QD[54] complexes are a combination of multiple pathways, direct membrane translocation, and endocytosis, respectively. The present results reveal that PR9/QD complexes colocalize with early endosomes and lysosomes after transduction delivery. This observation is consistent with our previous finding that PR9/QD complexes colocalize with F-actin and lysosomes,[51,54] while SR9/QD and HR9/QD complexes associate with neither.[49,51] Thus, the different uptake efficiencies may reflect different internalization routes.

5. CONCLUSIONS

We demonstrate that three arginine-rich CPPs (SR9, HR9, and PR9) interact with QDs to form stably noncovalent complexes *in vitro*. These CPPs enhance the delivery of associated QDs into human A549 cells. Zeta-potential and size analyses indicate the importance of electrostatic interactions between CPP/QD complexes and cytoplasmic membranes. CPP/QD complexes do not colocalize with mitochondria, nuclei, or ER, though some association with endosomes. Furthermore, CPPs are not cytotoxic when present at concentrations that efficiently promote cellular transduction.

ABBREVIATIONS

CPP	Cell-penetrating peptide
DMSO	Dimethyl sulfoxide
EEA1	Early endosome antigen 1
FITC	Fluorescein isothiocyanate
HR9	Histidine-rich nona-arginine
Pas	Penetration accelerating sequence
PR9	Pas nona-arginine
PBS	Phosphate buffered saline
QD	Quantum dot
R8	Octa-arginine
R9	Nona-arginine
SD	Standard deviation
SR9	Synthetic nona-arginine
SRB	Sulforhodamine B.

Acknowledgments: We thank Chia-Liang Cheng (Department of Physics, National Dong Hwa University, Taiwan) for performing particle size and zeta-potential measurements. This work was supported by the Postdoctoral Fellowship NSC 102-2811-B-259-001 (to Betty R. Liu), the Grant Number NSC 101-2320-B-259-002-MY3 (to Han-Jung Lee) from the National Science Council of Taiwan, and the Grant Number NP-1002-PP-02 (to Hwei-Hsien Chen) from the National Health Research Institutes of Taiwan.

References and Notes

1. H. Mattoussi, G. Palui, and H. B. Na, *Adv. Drug Deliv. Rev*. 64, 138 (**2012**).
2. F. Chen and D. Gerion, *Nano Lett*. 4, 1827 (**2004**).
3. X. Michalet, F. F. Pinaud, L. A. Bentolila, J. M. Tsay, S. Doose, J. J. Li, G. Sundaresan, A. M. Wu, S. S. Gambhir, and S. Weiss, *Science* 307, 538 (**2005**).
4. Y. Choi, K. Kim, S. Hong, H. Kim, Y. J. Kwon, and R. Song, *Bioconjug. Chem*. 22, 1578 (**2011**).
5. D. R. Larson, W. R. Zipfel, R. M. William, S. W. Clark, M. P. Bruchez, F. W. Wise, and W. W. Webb, *Science* 300, 1434 (**2003**).
6. J. B. Delehanty, H. Mattoussi, and I. L. Medintz, *Anal. Bioanal. Chem*. 393, 1091 (**2009**).
7. A. Komoto, S. Maenosono, and Y. Yamaguchi, *Langmuir* 20, 8916 (**2004**).
8. W. T. Al-Jamal, K. T. Al-Jamal, P. H. Bomans, P. M. Frederik, and K. Kostarelos, *Small* 4, 1406 (**2008**).
9. H. Duan and S. Nie, *J. Am. Chem. Soc*. 129, 3333 (**2007**).
10. M. Green and P. M. Loewenstein, *Cell* 55, 1179 (**1988**).
11. A. D. Frankel and C. O. Pabo, *Cell* 55, 1189 (**1988**).
12. A. van den Berg and S. F. Dowdy, *Curr. Opin. Biotechnol*. 22, 888 (**2011**).
13. S. Futaki, H. Hirose, and I. Nakase, *Curr. Pharm. Des*. 19, 2863 (**2013**).
14. K. M. Wagstff and D. A. Jans, *Curr. Med. Chem*. 13, 1371 (**2006**).
15. M. Chang, J. C. Chou, and H. J. Lee, *Plant Cell Physiol*. 46, 482 (**2005**).
16. K. Liu, H. J. Lee, S. S. Leong, C. L. Liu, and J. C. Chou, *J. Plant Growth Regul*. 26, 278 (**2007**).
17. J. F. Li, Y. Huang, R. L. Chen, and H. J. Lee, *Anticancer Res*. 30, 2193 (**2010**).
18. C. Y. Lee, J. F. Li, J. S. Liou, Y. C. Charng, Y. W. Huang, and H. J. Lee, *Biomaterials* 32, 6264 (**2011**).
19. J. S. Liou, B. R. Liu, A. L. Martin, Y. W. Huang, H. J. Chiang, and H. J. Lee, *Peptides* 37, 273 (**2012**).
20. Y. H. Wang, C. P. Chen, M. H. Chan, M. Chang, Y. W. Hou, H. H. Chen, H. R. Hsu, K. Liu, and H. J. Lee, *Biochem. Biophys. Res. Commun*. 346, 758 (**2006**).
21. M. Chang, J. C. Chou, C. P. Chen, B. R. Liu, and H. J. Lee, *New Phytol*. 174, 46 (**2007**).
22. C. P. Chen, J. C. Chou, B. R. Liu, M. Chang, and H. J. Lee, *FEBS Lett*. 581, 1891 (**2007**).
23. Y. H. Wang, Y. W. Hou, and H. J. Lee, *J. Biochem. Biophys. Methods* 70, 579 (**2007**).
24. Y. W. Hou, M. H. Chan, H. R. Hsu, B. R. Liu, C. P. Chen, H. H. Chen, and H. J. Lee, *Exp. Dermatol*. 16, 999 (**2007**).
25. B. R. Liu, J. C. Chou, and H. J. Lee, *J. Membr. Biol*. 222, 1 (**2008**).
26. Y. H. Dai, B. R. Liu, H. J. Chiang, and H. J. Lee, *Gene* 489, 89 (**2011**).
27. Y. J. Chen, B. R. Liu, Y. H. Dai, C. Y. Lee, M. H. Chan, H. H. Chen, H. J. Chiang, and H. J. Lee, *Gene*, 493, 201 (**2012**).
28. B. R. Liu, M. D. Lin, H. J. Chiang, and H. J. Lee, *Gene*, 505, 37 (**2012**).
29. B. R. Liu, Y. W. Huang, H. J. Chiang, and H. J. Lee, *Adv. Stu. Biol*. 5, 11 (**2013**).
30. M. J. Liu, J. C. Chou, and H. J. Lee, *Adv. Stu. Biol*. 5, 71 (**2013**).
31. B. R. Liu, Y. W. Huang, and H. J. Lee, *BMC Microbiol*. 13, 57 (**2013**).
32. J. W. Hu, B. R. Liu, C. Y. Wu, S. W. Lu, and H. J. Lee, *Peptides* 30, 1669 (**2009**).
33. S. W. Lu, J. W. Hu, B. R. Liu, C. Y. Lee, J. F. Li, J. C. Chou, and H. J. Lee, *J. Agric. Food Chem*. 58, 2288 (**2010**).
34. J. S. Wadia and S. F. Dowdy, *Curr. Opin. Biotechnol*. 13, 52 (**2002**).
35. S. Deshayes, M. C. Morris, G. Divita, and F. Heitz, *Cell. Mol. Life Sci*. 62, 1839 (**2005**).
36. Y. Wei, N. R. Jana, S. J. Tan, and J. Y. Ying, *Bioconjug. Chem*. 20, 1752 (**2009**).
37. H. D. Herce, A. E. Garcia, J. Litt, R. S. Kane, P. Martin, N. Enrique, A. Rebolledo, and V. Milesi, *Biophys. J*. 97, 1917 (**2009**).
38. S. L. Lo and S. Wang, *Biomaterials* 29, 2408 (**2008**).
39. K. Takayama, I. Nakase, H. Michiue, T. Takeuchi, K. Tomizawa, H. Matsui, and S. Futaki, *J. Control. Release* 138, 128 (**2009**).
40. Y. Ueda, F. Y. Wei, T. I. Hide, H. Michiue, K. Takayama, T. Kaitsuka, H. Nakamura, K. Makino, J. Kuratsu, S. Futaki, and K. Tomizawa, *Biomaterials* 33, 9061 (**2012**).
41. B. R. Liu, Y. W. Huang, H. J. Chiang, and H. J. Lee, *J. Nanosci. Nanotech*. 10, 7897 (**2010**).
42. Y. Wei, N. R. Jana, S. J. Tan, and J. Y. Ying, *Bioconjug. Chem*. 20, 1752 (**2009**).
43. P. Guterstam, F. Madani, H. Hirose, T. Takeuchi, S. Futaki, S. El-Andaloussi, A. Graslund, and U. Langel, *Biochim. Biophys. Acta*, 1788, 2509 (**2009**).
44. A. Hoshino, K. Fujioka, T. Oku, S. Nakamura, M. Suga, Y. Yamaguchi, K. Suzuki, M. Yasuhara, and K. Yamamoto, *Microbiol. Immunol*. 48, 985 (**2004**).
45. F. L. Xue, J. Y. Chen, J. Guo, C. C. Wang, W. L. Yang, P. N. Wang, and D. R. Lu, *J. Fluoresc*. 17, 149 (**2007**).
46. Y. E. Koshman, S. B. Waters, L. A. Walker, T. Los, P. de Tombe, P. H. Goldspink, and B. Russell, *J. Mol. Cell. Cardiol*. 45, 853 (**2008**).
47. B. R. Liu, J. F. Li, S. W. Lu, H. J. Lee, Y. W. Huang, K. B. Shannon, and R. S. Aronstam, *J. Nanosci. Nanotechnol*. 10, 6534 (**2010**).
48. Y. Xu, B. R. Liu, H. J. Lee, K. B. Shannon, J. G. Winiarz, T. C. Wang, H. J. Chiang, and Y. W. Huang, *J. Biomed. Biotechnol*. 2010, 948543 (**2010**).
49. B. R. Liu, Y. W. Huang, J. G. Winiarz, H. J. Chiang, and H. J. Lee, *Biomaterials* 32, 3520 (**2011**).
50. Y. W. Huang, H. J. Lee, B. R. Liu, H. J. Chiang, and C. H. Wu, *Methods Mol. Biol*. 991, 249 (**2013**).

51. B. R. Liu, H. J. Chiang, Y. W. Huang, M. H. Chan, H. H. Chen, and H. J. Lee, *Pharm. Nanotechnol.* 1, 151 **(2013)**.
52. B. R. Liu, J. S. Liou, Y. J. Chen, Y. W. Huang, and H. J. Lee, *Mar. Biotechnol.* (*NY*) 15, 584 **(2013)**.
53. B. R. Liu, J. S. Liou, Y. W. Huang, R. S. Aronstam, and H. J. Lee, *PLoS One* 8, e64205 **(2013)**.
54. B. R. Liu, S. Y. Lo, C. C. Liu, C. L. Chyan, Y. W. Huang, R. S. Aronstam, and H. J. Lee, *PLoS One* 8, e67100 **(2013)**.
55. B. R. Liu, J. G. Winiarz, J. S. Moon, S. Y. Lo, Y. W. Huang, R. S. Aronstam, and H. J. Lee, *Colloids Surf. B Biointerfaces* 111, 162 **(2013)**.
56. I. Nakase, S. Kobayashi, and S. Futaki, *Biopolymers* 94, 763 **(2010)**.
57. F. Madani, S. Lindberg, U. Langel, S. Futaki, and A. Graslund, *J. Biophys*. 2011, 414729 **(2011)**.
58. S. D. Conner and S. L. Schmid, *Nature* 422, 37 **(2003)**.
59. H. Hirose, T. Takeuchi, H. Osakada, S. Pujals, S. Katayama, I. Nakase, S. Kobayashi, T. Haraguchi, and S. Futaki, *Mol. Ther*. 20, 984 **(2012)**.
60. T. Takeuchi, M. Kosuge, A. Tadokoro, Y. Sugiura, M. Nishi, M. Kawata, N. Sakai, S. Matile, and S. Futaki, *ACS Chem. Biol*. 1, 299 **(2006)**.

Received: 30 August 2013. Accepted: 13 October 2013.